Available online at www.sciencedirect.com
ScienceDirect
International Journal of Heat and Mass Transfer 51 (2008) 4439–4446
International Journal of HEAT and MASS TRANSFER
www.elsevier.com/locate/ijhmt

Effect of surface property of molten metal pools on triggering of vapor explosions in water droplet impingement

M. Furuya *, T. Arai

Nuclear Technology Research Laboratory, Central Research Institute of Electric Power Industry, 2-11-1 Iwado-kita, Komae, Tokyo 201-8511, Japan

Received 20 April 2007; received in revised form 19 December 2007
Available online 13 April 2008

Abstract

Small-scale experiments have been conducted to investigate the triggering mechanism of vapor explosions. In order to attain good repeatability and visibility, a smooth round water droplet was impinged onto a molten alloy surface. This configuration suppresses premixing events prior to triggering.

Six molten metal and alloys were used as the pool liquid. The lower limit of the contact temperature in the vapor explosion region closely agrees with the spontaneous bubble nucleation temperature of water. The upper limit of the initial molten alloy temperature decreases when an oxide layer forms on the surface causing an increase of the emissivity of thermal radiation that has a stabilizing effect on the vapor film. When an oxide layer was formed on the surface, a water droplet was occasionally entrapped into a molten alloy dome, since the oxide layer prevents the droplet from evaporating coherently. The vapor explosion region obtained for the mirror surface is a conservative estimate, since that for the oxide surface fell into the internal region of the vapor explosion for the mirror surface.

Keywords: Vapor explosion; Triggering; Liquid–liquid direct contact; Spontaneous bubble nucleation; Fragmentation

1. Introduction

A large-scale vapor explosion is generally considered to involve the following four stages shown in Fig. 1: (1) coarse mixing, (2) triggering, (3) propagation, and (4) expansion. Triggering is the event of direct contact between a high temperature liquid (e.g., a molten alloy) and a low temperature volatile liquid (e.g., water) that initiates the rapid, local heat transfer and pressure rise. Fletcher [4] well reviewed the role of triggering in vapor explosions in terms of nuclear reactor safety. In the other industries such as metallurgy and the paper industry, investigation of vapor explosions is of importance from the point of view of safety as well. In spite of the industrial relevance, knowledge of the triggering mechanism is still insufficient even for a simple molten alloy droplet system.

At triggering, the vapor film surrounding a hot-liquid collapses to allow hot and cold-liquids to contact each other. It is well known that there are two different collapse modes. One is where an external force acts on the vapor film, i.e., the arrival of an external pressure wave and/or shear stress due to velocity difference. The other involves an internal factor, i.e., thermal balance between evaporation and condensation. The latter is called self-triggering.

In the past forty years, there have been a number of experiments [1–3,9,11] using several grams of molten tin immersed in a water pool to investigate the self-triggering conditions.

Due to the random nature of vapor explosions, experimental data are not reproducible even if initial conditions are set to be identical. The authors believe that the random nature is caused by three factors that change sensitivity to the trigger events in the premixing stage: (1) heat transfer rate from a hot to a cold fluid, (2) orientation of gravity force direction and the interface direction to the triggering events, and (3) surface property, i.e., the oxide layer formation. The

* Corresponding author. Tel.: +81 3 3480 2111; fax: +81 3 3480 2493.
E-mail address: furuya@criepi.denken.or.jp (M. Furuya).

0017-9310/$ - see front matter © 2008 Elsevier Ltd. All rights reserved.
doi:10.1016/j.ijheatmasstransfer.2008.02.025

Nomenclature

Alphabets

D	water droplet diameter (m)
P_s	system pressure (Pa)
T_{cr}	critical temperature of water (°C)
T_d	initial temperature of a water droplet (°C)
T_{hn}	homogeneous bubble nucleation temperature of water (°C)
T_i	contact temperature based on the conduction theory (°C)
T_m	initial temperature of a molten alloy pool (°C)
T_{mp}	melting temperature (°C)
We	impingement Weber number

Greek symbol

τ_d	dwell time (s)

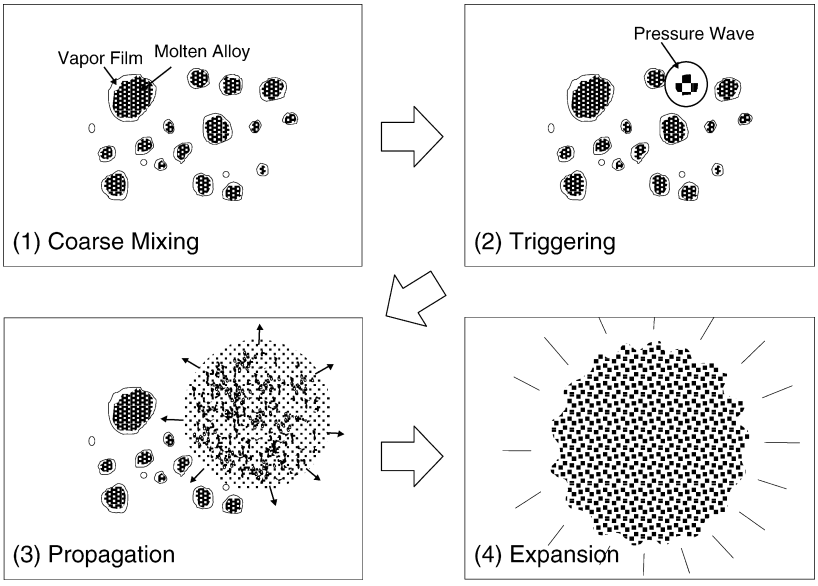

Fig. 1. Four conceptual stages of the large-scale vapor explosion.

authors have performed the droplet impingement experiment to suppress the premixing stage. In this experiment, vapor explosion occurred a few milliseconds after a water droplet had impinged onto the molten alloy surface. Experiments had been conducted thereby changing initial temperatures and surface conditions before the contact. Those parameter effects on the triggering event can be investigated directly without any interference with the premixing stage.

Fig. 2 shows an evaporation time against initial temperature of pool liquid in the droplet impingement system. The evaporation phenomena is classified into four states:

Wetting state: A hemispherical droplet sits on and touches the molten alloy pool surface. It evaporates from the free surface of the droplet. Boiling is observed if the molten alloy temperature is high.

Transition state: The intermediate condition between the wetting and the spheroidal state. Bouncing motion can be observed due to intermittent contact with the molten alloy pool surface.

Spheroidal state: A spheroidal droplet exists above the molten alloy pool surface. The evaporation time is long since a vapor film between the droplet and pool liquid surface prevents the droplet from being in contact with the surface.

Vapor explosion: Deformation of the molten alloy pool surface is induced by strong thermal interaction. Vapor explosion can be seen only if the pool material is a liquid.

Another unique phenomenon was frequently observed when an oxide layer was formed on the molten alloy surface. This phenomenon was examined later using high-speed video frames. The authors have visualized [5] the spreading process of spontaneous bubble nucleation immediately after a droplet came into contact with a molten alloy surface, using video frames at an exposure time of 100 ns. The authors have also investigated the effects of the droplet subcooling and system pressure on the triggering conditions.

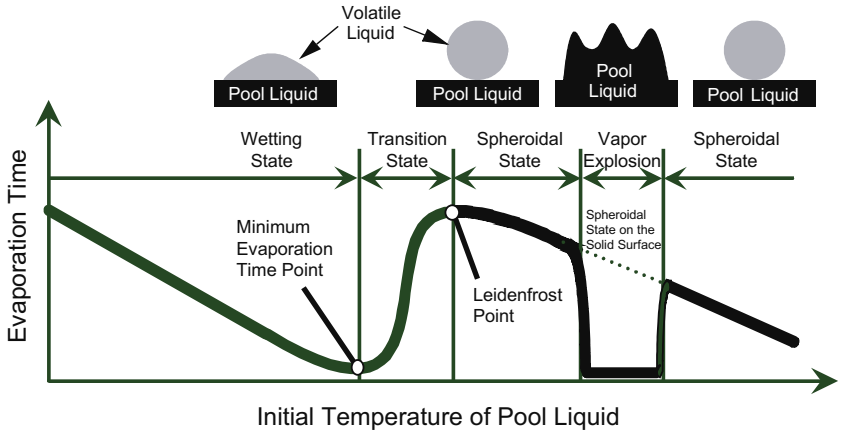

Fig. 2. Representative evaporation curve.

It is widely known [10,8,7] that the conditions of vapor explosion differ from material to material – e.g., a tin droplet explodes spontaneously in a water pool, but a zinc droplet does not. This may be caused by the differences in heat transfer and mixing conditions in the premixing stage.

In the present study, a smooth round water droplet was impinged onto a molten alloy surface. The droplet impingement system allows approximately identical initial conditions in the premixing stage to investigate the triggering conditions for different materials, because the triggering can occur a few milliseconds after the impingement.

This paper addresses contact mode maps as the triggering conditions for six different kinds of materials and the effect of an oxide layer formed on the molten alloy surface based on high-speed video frames.

2. VECTOR experimental facility and experimental procedures

Fig. 3 shows a schematic of the VECTOR (vapor explosion of CRIEPI test with oxide layer removal devices) facility. The containment vessel has a volume of 0.48 m^3 and contains a droplet nozzle, a molten alloy crucible and devices to remove the oxide layer. The molten alloys used were lead–bismuth, lead, bismuth, tin, zinc, and indium. The internal dimensions of the crucible are 150 mm in length, 170 mm in width, and 30 mm in depth. Temperatures were measured at 2 mm-depth intervals in the molten alloy pool, and were found to show scatter within 0.7 K due to natural convection. Type-K thermocouples were immersed into the molten alloy pool in a depth of 8 mm to measure the initial molten alloy temperature.

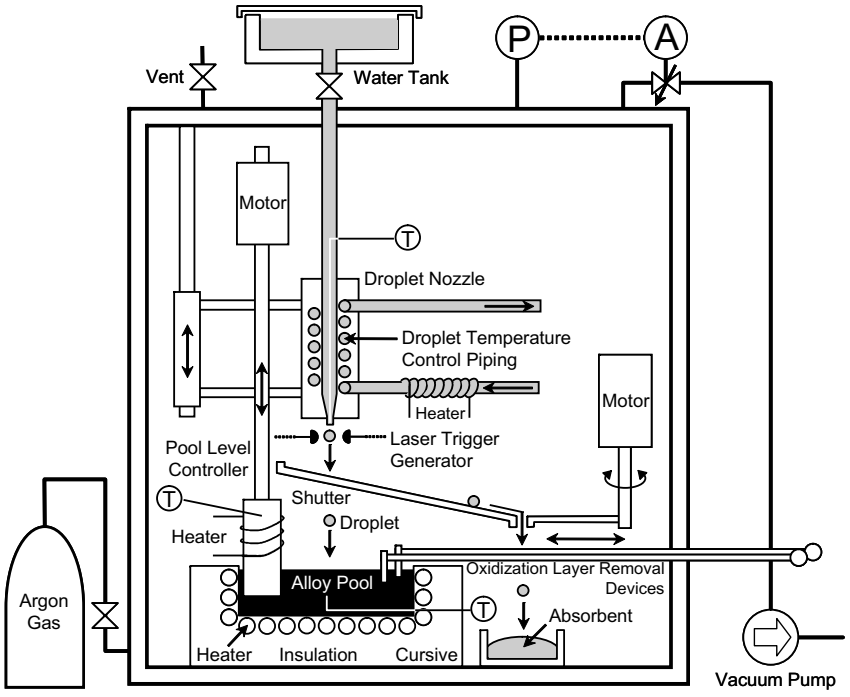

Fig. 3. Schematic of VECTOR facility.

Degassed water that passed through an ion exchange resin was used as the impingement droplet. A smooth, round water droplet was released slowly from the droplet nozzle by the gravity head. Type-K thermocouples were inserted into the nozzle and attached at the nozzle exit to measure the initial droplet temperature. The temperature of water in the nozzle was maintained at a desired value by controlling the flow rate and the temperature of water in the droplet temperature control piping.

Although air inside the containment vessel was completely replaced by argon, a thin oxide layer was formed on the molten alloy pool surface due to the presence of small amounts of steam and oxygen. Devices to remove the oxide layer were operated in two directions to scrape off the oxide layer. In order to investigate a surface oxidation effect, a dwell time (τ_d) to impingement after the scraped off of the oxide layer was varied in this experiment.

There were two types of the molten alloy surfaces: mirror and oxide surfaces. The term 'mirror surface' means that to the condition under which a droplet impinged onto the molten alloy surface immediately after the removal of the oxide layer on the pool surface. On the contrary, the word 'oxide surface' means that the pool surface was covered with a thin oxide layer ten seconds after the removal of the oxide layer. The same surface conditions could be reproduced at the same dwell time (τ_d) for the same material and its temperature by injecting argon gas into the containment vessel at a constant rate. One should realize that actual surface conditions varied with the thermo-physical properties of materials and the temperature. The oxide layer was at a slightly frosted glass condition for lead–bismuth alloy at a dwell time of 10 s.

A series of images were taken using a high-speed digital video camera (model SpeedCam-512 by Weinberger AG Inc). Common experimental conditions in the present experimental series were the system pressure of 0.1 MPa, the impingement Weber number of 106, and the droplet diameter of 4.5 mm.

An error in measuring the temperatures was estimated to be 0.7 K. Uncertainty of time point was around 0.2 ms for given video frames. For more fine time resolution, consult previous papers [5] which addressed the spontaneous bubble nucleation and the water droplet fragmentation processes video-framed at 0.01 ms intervals.

3. Experimental results and discussion

3.1. Visual observations

Fig. 4 shows four series of frames for (a) the wetting state at the minimum evaporation time point, (b) the spheroidal state, (c) vapor explosion, and (d) droplet entrapping. Initial conditions were identical for all series except the initial lead–bismuth temperature. The initial water droplet temperature was set to 70 °C.

Note that only one droplet in each frame touched the molten alloy surface at 0 ms and was clearly reflected in the molten alloy pool. Before 1 ms, these four sets of frames show the similar deformation process. The third frame (2 ms) in Fig. 4c, however, shows a drastic change with a sudden occurrence of explosive fragmentation of the whole droplet. At the same time, filaments of the molten alloy rose up to be in a crown shape. After that, the center portion was raised, as shown in the frame at 80 ms. The vapor explosion was significantly different from the wetting and the spheroidal state in which no ripples can be seen throughout the evaporation process. After the vapor explosion, spherical particles of molten alloy having a diameter of less than 0.5 mm splashed at the corner of the containment vessel at a distance of about 600 mm from the impingement point.

When the surface was oxidized, a unique phenomenon was often observed, as shown in Fig. 4d. Compared to the filaments in the vapor explosion shown in Fig. 4c, a limited amount of the water hemisphere evaporated resulting in the formation of small ripples, as shown at 2 ms. Subsequently, an unevaporated water droplet was entrapped in a molten alloy dome. When vapor produced collapsed the molten alloy dome under the film boiling condition at 67 ms, the entrapped water droplet emerged from the dome (not shown here, see the droplet at 80 ms). Hereafter, this phenomenon is called 'droplet entrapping.' As shown in Fig. 4c at 2 ms, the droplet was evaporated coherently on the mirror surface. On the contrary, the oxide layer may occasionally prevent the droplet from evaporating coherently as shown in Fig. 4c at 2 ms, resulting in droplet entrapping. In this respect, oxide layer formation is one of the reasons why vapor explosion exhibits a random nature and causes a loss of repeatability.

3.2. Triggering conditions

3.2.1. Effect of surface property

Fig. 5a–c are contact mode maps of initial water droplet and molten lead–bismuth temperature. Each set of conditions was classified into five different states (see Figs. 2 and 4). Fig. 5a and b were obtained for the mirror surface and the oxide surface, respectively.

As shown in Fig. 5a, there is a definite vapor explosion region surrounded by the spheroidal state (film boiling) region due to a suppression of the premixing stage in this configuration. The two curves in the figure indicate the conditions under which the contact temperature at the interface, T_i, agrees with the homogeneous bubble nucleation temperature, T_{hn}, and critical temperature, T_{cr}, of water. The contact temperature was estimated based on the conduction theory of two semi-infinite solid bodies in contact with each other, as follows:

$$T_i = \frac{\sqrt{\rho_m Cp_m \lambda_m} T_m + \sqrt{\rho_d Cp_d \lambda_d} T_d}{\sqrt{\rho_m Cp_m \lambda_m} + \sqrt{\rho_d Cp_d \lambda_d}}, \quad (1)$$

where ρ, Cp and λ denote density, thermal capacity at a constant pressure, and thermal conductivity, respectively. The

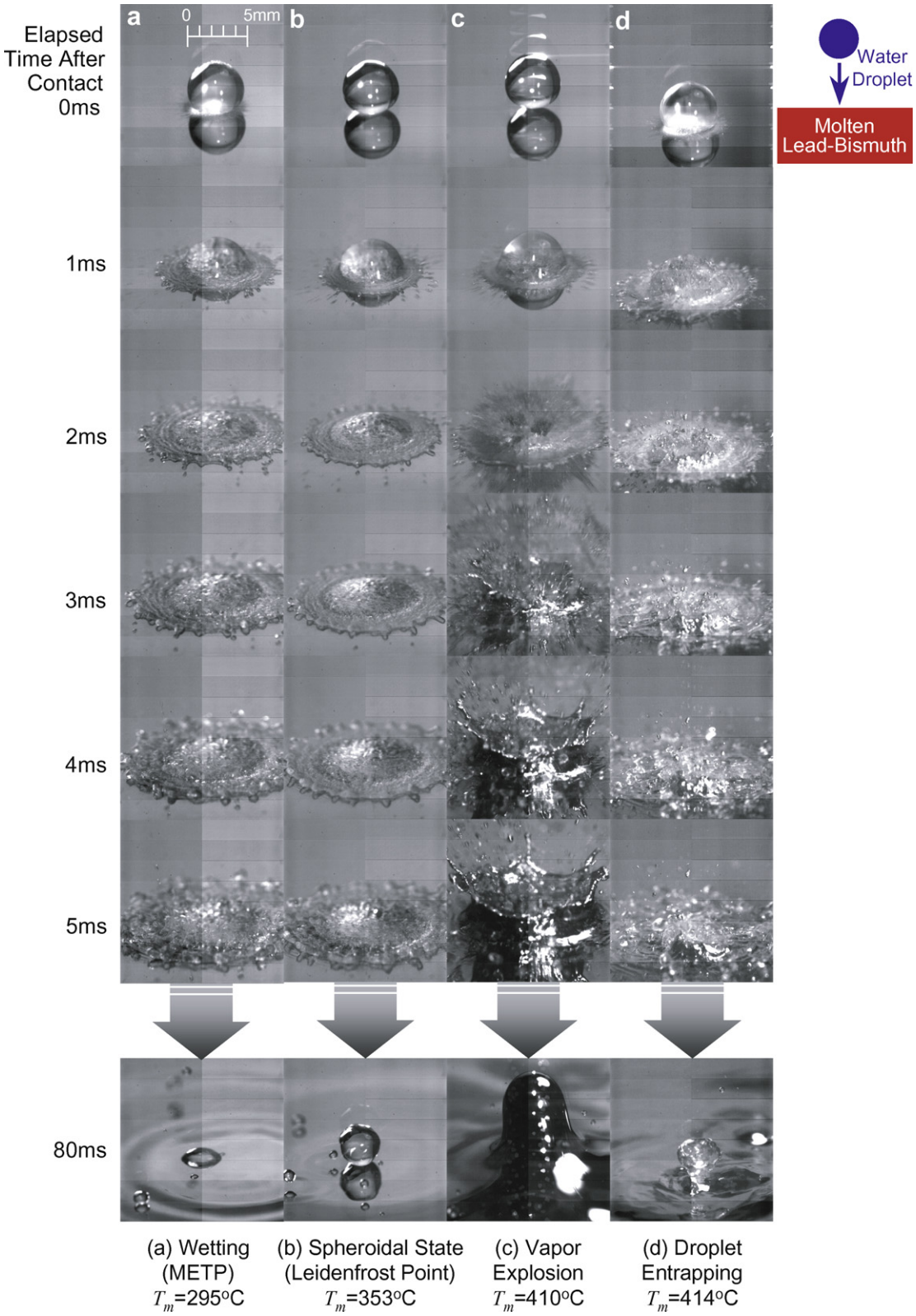

Fig. 4. Series of frames illustrating contact modes for water droplet – molten lead–bismuth pool system.

subscripts m and d indicate the molten alloy and the liquid droplet, respectively. According to the boundary between vapor explosion and the spheroidal state regions, vapor explosions seem to occur when the water is sufficiently subcooled to suppress the formation of a vapor film, and when the contact temperature is higher than the spontaneous

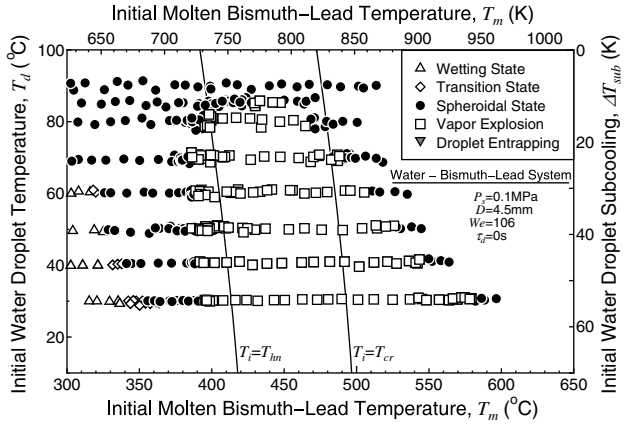

(a) Mirror Surface ($\tau_d = 0$ s)

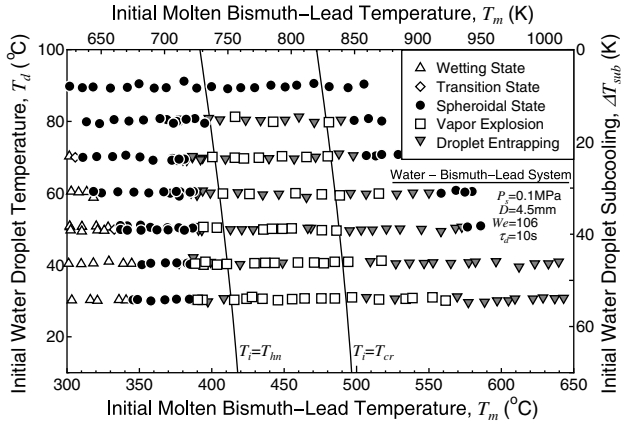

(b) Oxidized Surface ($\tau_d = 10$ s)

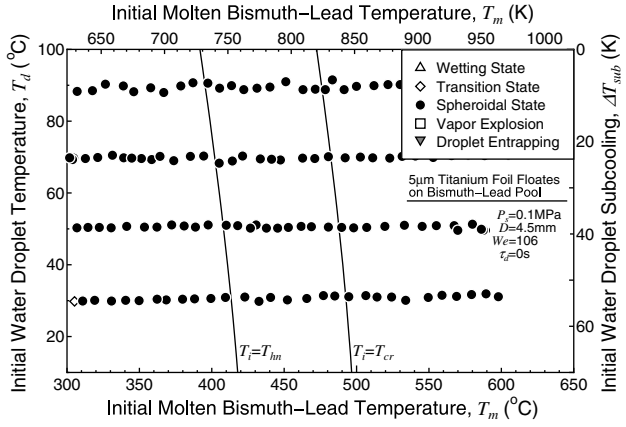

(c) Titanium Foil

Fig. 5. Contact mode maps in terms of surface property for water droplet – molten lead–bismuth pool system.

bubble nucleation temperature. The suppression of the vapor film can be estimated as a function of the molten alloy temperature by the vapor film collapse model [6]. According to the model, the upper limit decreases with an increase of the emissivity of thermal radiation by stabilizing the vapor film between the molten alloy and water droplet. A list of materials in increasing order of the emissivity is: indium, tin, lead, bismuth–lead, and bismuth. The list is coincide with that in decreasing order of the upper limit temperature where the vapor explosion occurs. When the surface is oxidized, the emissivity further increases, causing an enhancement the stability of the vapor film. The upper limit does therefore, decrease when an oxide layer formed on the surface.

On the other hand, droplet entrapping occurred frequently on the oxide surface. Vapor explosion for the oxide surface occurred in the internal region of the vapor explosion for the mirror surface. Thus, the vapor explosion

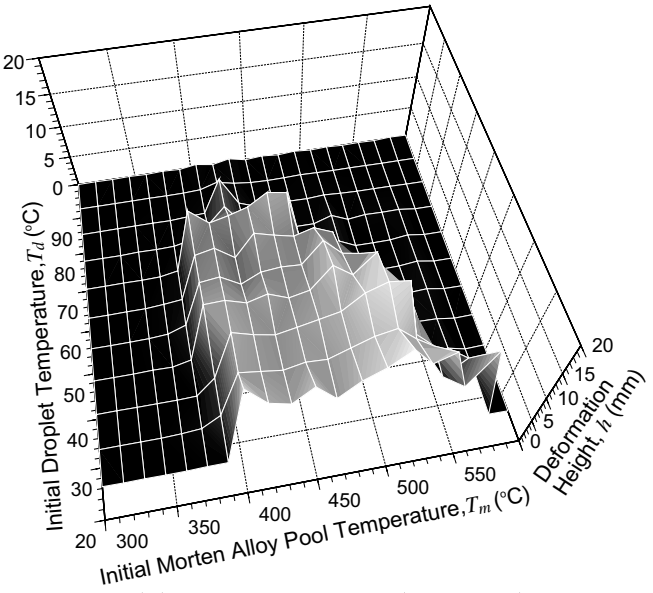

(a) Mirror Surface ($\tau_d = 0$ s)

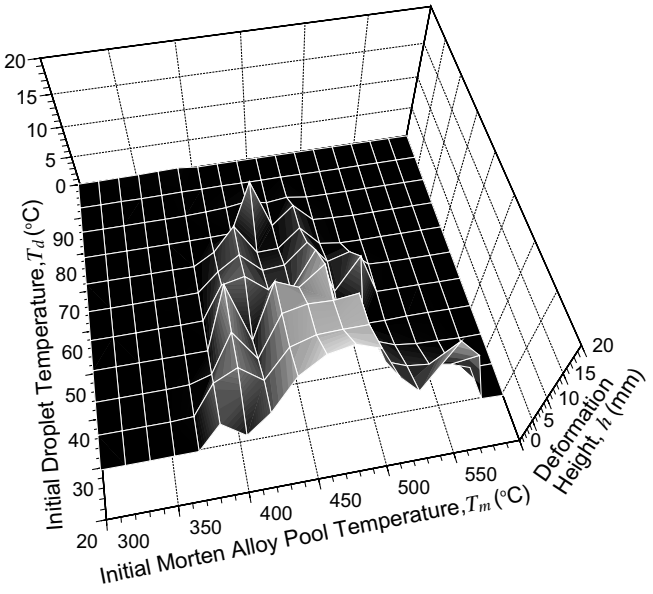

(b) Oxidized Surface ($\tau_d = 10$ s)

Fig. 6. Maximum deformation height in terms of surface property.

Table 1
Maximum deformation height statistics counting for vapor explosion data

Pool material	Bismuth–lead		Tin		Lead		Zinc		Indium		Bismuth
Dwell time, τ_d (s)	0	10	0	10	0	10	0	10	0	10	0
Number of explosion data	137	55	74	43	56	20	0	0	44	71	125
Average (mm)	12.6	13.3	16.0	18.2	15.8	16.9	0.0	0.0	14.5	14.5	15.2
Standard deviation (mm)	3.2	4.1	4.9	4.7	3.4	2.3	–	–	4.6	4.2	3.7

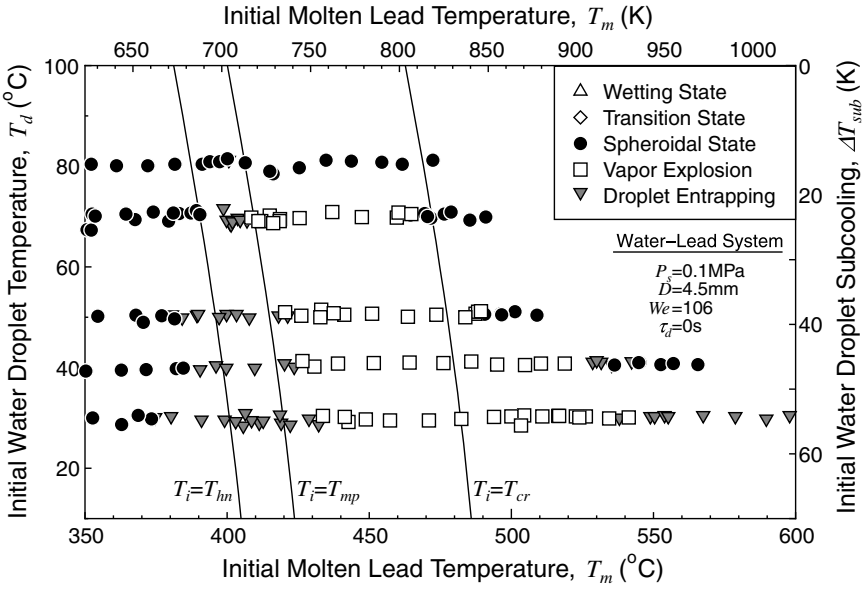

Fig. 7. Contact mode map for lead.

region determined for the mirror surface would be a conservative estimate.

Vapor explosion and droplet entrapping cannot occur on a solid surface, however, the observed oxide layer should be in the solid film within such a low lead–bismuth alloy temperature range. In order to investigate the difference between a thin foil and an oxide layer, five-micrometer-thick titanium foil was placed on the molten alloy pool. As shown in Fig. 5c, vapor explosion and droplet entrapping were not observed on the floating foil. Although experiments are repeated for one-micrometer-thick titanium foil instead of titanium foil was placed on the molten alloy pool, vapor explosion and droplet entrapping were not observed. It can be concluded that even a weak shear disturbance could tear off the thin oxide layer to appear a fresh surface, though it was hard to break the metal foil.

Fig. 6 shows the experimental result with lead–bismuth for the maximum deformation height with respect to both initial temperatures. The maximum deformation height was measured from a digital image at the center portion after a crown shape descended (see Fig. 4c at 80 ms). The height became lower with increasing the initial droplet temperature. Statistics of the maximum deformation height are summarized in Table 1. The average deformation height for the oxide surface was higher than that for the mirror surface. This is because droplet entrapping is likely to occur at a higher molten alloy temperature with higher droplet temperature on the oxide surface, where the maximum deformation height was relatively low.

3.2.2. Effect of thermo-physical property

Fig. 7 shows a contact mode map for the mirror surface of lead. The melting point of lead, T_{mp} (=327.6 °C), is higher than the homogeneous bubble nucleation temperature but lower than the critical temperature of water. When the contact temperature was below the melting temperature of lead, droplet entrapping was observed in place of vapor explosion. Solidification may prevent lead from the fine fragmentation that enhances the heat transfer to water. The lower boundary of the droplet entrapping region agrees with the spontaneous bubble nucleation temperature.

Fig. 8 shows vapor explosion regions for the mirror surface of six different materials: lead–bismuth, bismuth, lead, tin, indium, and zinc. Only the spheroidal state was observed in the experiment using zinc for $T_{mp} < T_m <$ 520 °C and 13 °C $< T_d <$ 52 °C. Although air inside the containment vessel was replaced by argon, the presence of steam and oxygen allowed the zinc pool surface to form a relatively thick flake like oxide layer, resulting in the absence of vapor explosion and droplet entrapping regions. On the contrary, contact mode maps for the mirror and

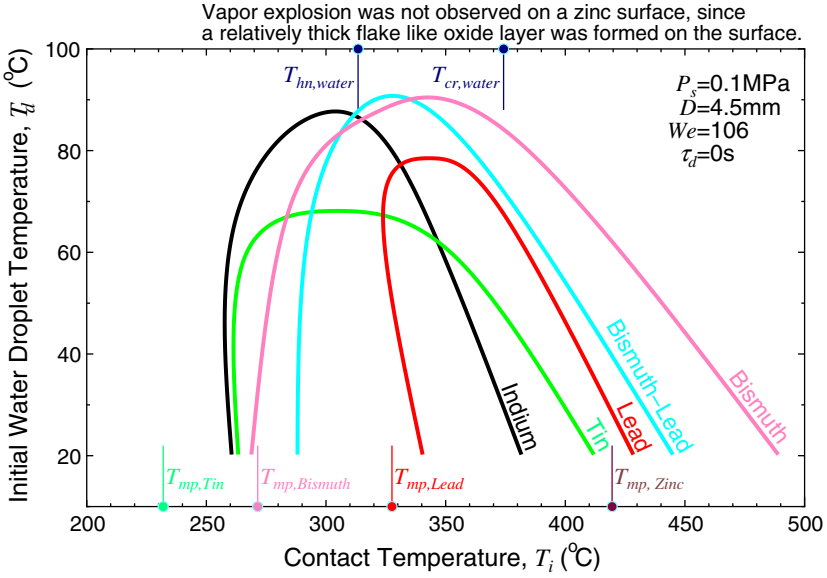

Fig. 8. Vapor explosion regions for different pool materials.

oxide surfaces of indium were similar to each other (see also the statistics in Table 1), though a slightly reddish brown thin oxide layer was formed immediately on both surfaces above 350 °C.

4. Conclusions

The following conclusions were drawn from the result of the contact mode maps obtained in the water droplet impingement experiments for six different materials.

(1) Droplet entrapping was frequently observed on the oxide surface in the internal region of vapor explosion for a mirror surface. A water droplet was entrapped in a molten alloy dome, since an oxide layer prevented the water droplet from evaporating coherently.
(2) Vapor explosion was not observed on a zinc surface since a relatively thick flake like oxide layer was formed on the surface.
(3) The lower limit of the contact temperature in the vapor explosion region agrees with the spontaneous bubble nucleation temperature of water or the melting point of the alloy.
(4) The upper limit decreases when an oxide layer formed on the surface causing an increase of the emissivity of thermal radiation that has a stabilizing effect on the vapor film.
(5) The vapor explosion region for the mirror surface is a conservative estimate since that for the oxide surface falls into an internal region of the vapor explosion for the mirror surface.

Acknowledgements

The authors are grateful for many constructive suggestions made by Emeritus Professor Akira Inoue of Tokyo Institute of Technology. Thanks to Mr. Masatake Fujie of Electric Power Techno Systems Co., Ltd for helping these experiments.

References

[1] R. Akiyoshi, S. Nishio, I. Tanazawa, Trans. JSME, Ser. B 54 (499) (1988) 630–635 (in Japanese).
[2] R.H. Bradley, L.C. Witte, Explosive interaction of molten metals injected into water, Nucl. Sci. Eng. 48 (1972) 387–396.
[3] T.A. Dullforce, D.J. Buchanan, R.S. Peckover, Self-triggering of small-scale fuel–coolant interaction: I. Experiments, J. Phys. D: Appl. Phys. 9 (1976) 1295–1303.
[4] D.F. Fletcher, A review of the available information on the triggering stage of a steam explosion, Nucl. Safety 35 (1) (1994) 36–57.
[5] M. Furuya, I. Kinoshita, Y. Nishi, Vapor explosion in the droplet impingement system, in: Proceedings of the 11th International Heat Transfer Conference, Kyongju, Korea 5, 1998, pp. 471–476.
[6] M. Furuya, K. Matsumura, I. Kinoshita, A linear stability analysis of a vapor film in terms of the triggering of vapor explosions, J. Nucl. Sci. Technol. 39 (10) (2002) 1026–1032.
[7] K. Miyazaki, O. Yamamoto, et al., Thermal interaction of water droplet with molten tin, J. Nucl. Sci. Technol. 21 (12) (1984) 907–918.
[8] M. Ochiai, S.G. Bankoff, A local propergation theory for vapor explosions. Third Specialist Mtg. on Sodium/Fuel Interaction in Fast Reactors, 1976, pp. 129–152.
[9] M. Shoji, N. Takagi, Trans. JSME, Ser. B 48 (433) (1982) 1768–1774 (in Japanese).
[10] M. Shoji, N. Takagi, thermal interaction when a cold volatile liquid droplet impinges on a hot liquid surface, Bull. JSME 29 (250) (1986) 1183–1187.
[11] L.C. Witte, T.J. Vyas, A.A. Gelabert, Heat transfer and fragmentation during molten-metal/water interactions, Trans. ASME J. Heat Transfer 95 (1973) 521–527.